JANUARY 04 2024

Impact of the ear canal motion on the impedance boundary conditions in models of the occlusion effect

Simon Kersten ; Franck Sgard ; Michael Vorländer

J. Acoust. Soc. Am. 155, 56–67 (2024)
https://doi.org/10.1121/10.0024244

JASA ARTICLE

Impact of the ear canal motion on the impedance boundary conditions in models of the occlusion effect

Simon Kersten,[1,a] Franck Sgard,[2] and Michael Vorländer[1]
[1]Institute for Hearing Technology and Acoustics, RWTH Aachen University, 52074 Aachen, Germany
[2]Direction de la Recherche, Institut de Recherche Robert-Sauvé en Santé et Sécurité du Travail (IRSST), Montréal, Québec, H3A 3C2, Canada

ABSTRACT:
The occlusion effect (OE) denotes the increased low-frequency perception of bone-conducted sounds when the ear canal (EC) is occluded. Circuit and finite element (FE) models are commonly used to investigate the OE and improve its prediction, often applying acoustic impedances at the EC entrance and tympanic membrane (TM). This study investigates the sound generation caused by the structural motion of the EC. In addition to the EC wall vibration, it accounts for the motions of the EC entrance and TM, resulting from nondeforming motion of the surrounding structures. A model extension including these motions with the impedances is proposed. Related mechanisms are illustrated based on a circuit model. Implications are discussed by using an EC motion extracted from a FE model of a human head. The results demonstrate that the motions of the EC entrance and TM, addressed by the proposed extension, affects the TM sound pressure and may lead to a reduction of the OE at lower frequencies compared to solely considering the EC wall vibration. Accordingly, this phenomenon potentially reconciles differences between experimental data and OE simulations at frequencies below about 250 Hz, highlighting the importance to discern between multiple contributing mechanisms to the TM sound pressure.
 https://doi.org/10.1121/10.0024244
(Received 28 July 2023; revised 8 December 2023; accepted 13 December 2023; published online 4 January 2024)
[Editor: James F. Lynch] Pages: 56–67

I. INTRODUCTION

The occlusion effect (OE) denotes the increased low-frequency perception of bone-conducted (BC) sounds, resulting from the occlusion or blockage of the ear canal (EC) with devices such as earplugs or hearing aids.[1] This phenomenon manifests in the amplification of physiological noise and alterations of one's own voice perception. The OE contributes to the discomfort experienced by workers who wear earplugs,[2] and it can diminish the overall acceptance of hearing aids among their users.[3]

The OE is objectively measurable as the sound pressure level difference in the EC due to the occlusion. The OE exhibits a low-pass characteristic[4–6] and mainly appears at frequencies below 1 kHz.[7] In contrast to air-conducted sound, which enters the EC at its entrance, the OE is a result of the structural transmission of BC sound. Hence, the sound pressure in the EC is in the open and occluded case induced by the moving EC boundaries. Influencing factors on this phenomenon are as follows:

- the frequency-dependent distribution of the EC wall vibrations in magnitude and phase,[8,9] which varies between the elastic soft tissue/cartilage part and bony part of the EC;[5]
- the different areas and orientations of the EC wall, EC entrance, and tympanic membrane (TM)[10,11] in relation to the direction of the motion;
- the source of the BC stimulation, e.g., BC transducers,[5,12–14] one's own voice,[15,16] or mastication;[16]
- the variation of the vibrating area of the wall with the occluding device's insertion;[3,5]
- the mechanical load of the occluding device to the vibration of the EC wall;[3,15,17]
- the acoustical load to the vibration of the EC wall due to the occlusion;[18] and
- the boundary and loading conditions within numerical simulations, e.g., at the temporal bone and soft tissue of an outer ear model[8] or at the base of a truncated head model.[19]

Researchers have employed various modeling approaches to simulate the OE, ranging from one-dimensional circuit models (e.g., Refs. 5, 6, 8, 15, 20, and 21) to more complex finite element (FE) models (e.g., Refs. 8, 13, 18, 19, and 22). It is a common approach within OE models to represent the sound radiation at the open EC entrance by an acoustic impedance.[5,6,8,13,15,18,20,22] Similarly, also the occluding device can be considered as an impedance at the EC entrance, which differs from the open-ear case. In several OE models, such an impedance is incorporated explicitly in at least one of the investigated conditions.[5,6,8,13,15,18,20]

[a]Email: simon.kersten@akustik.rwth-aachen.de

https://doi.org/10.1121/10.0024244

At the TM, the impedance represents the load by the membrane itself, the middle ear (ME) cavity, the ME ossicles, and inner ear (see, e.g., Shaw and Stinson[23] or Hudde and Engel[24–26]) Using such an impedance allows bypassing the necessity of modeling the ME structures in detail, therefore, it is the most common approach for OE models.[5,6,8,13,15,18–22]

Conceptually, the impedance approach assumes a piston-like motion at the entrance and TM.[27] Such a simplification is justified because the frequency range of interest extends up to a maximum of 2 kHz, hence, the wavelength in air is significantly larger than the radial dimensions of the EC and TM [e.g., with a speed of sound in air of 343 m/s, the wavelength at 2 kHz exceeds a typical TM diameter of about 9 mm (Ref. 28) by 19 times]. Furthermore, experimental observations suggest a "simple vibration pattern"[29] of the TM below 2 kHz. This allows treating its motion by means of a volume velocity instead of considering the spatially distributed point velocity.[29,30] The corresponding sound pressure level close to the TM varies spatially by about 1 dB within the considered frequency range.[31] The TM acoustic impedance can then be defined as the average sound pressure on the TM divided by the volume velocity of the TM during air-conducted stimulation.[28] It is worth noting that for BC stimulation, the TM may also play an active role by radiating sound originating from the ME into the EC. Experiments suggest that this reverse excitation does not significantly contribute to the EC sound pressure except at the EC resonance at approximately 3 kHz.[7]

Yet, predicting the OE and assessing the effectiveness of measures to reduce it, such as vents,[32] open-fitting hearing aids,[33] or sound-absorbing earplugs,[34,35] remains challenging.[8,19] Comparisons between experimental data and simulations[18,19,22] reveal an overestimation of the OE, particularly at frequencies below 250 Hz. Interestingly, experimental results also exhibit a higher variance of the OE and stronger excitation dependence in this frequency range.[12,16] Using a FE model of a human head, Xu *et al.*[19] highlighted that the radiation of the BC-stimulated head vibrations into the open EC could account for some of these observations. However, existing discrepancies between experimental and simulation data remain unexplained.

This study investigates whether considering a more comprehensive view on the three-dimensional structural motion of the EC could, at least partially, elucidate the discrepancies at low frequencies between the calculated and measured OEs. Below 300 Hz, the skull exhibits a rigid body motion,[36] which causes the part of the EC surrounded by bone to follow. Additionally, the wavelength in the surrounding soft tissue and cartilage is larger or similar to the dimensions of the EC. For instance, when employing the material parameters referred to as "reference" in Xu *et al.*,[19] the wavelength of shear waves in soft tissue at 100 Hz exceeds the EC dimensions by a factor of 3. In the case of cartilage, the wavelength surpasses the EC dimensions even by a factor of 20–40 at this frequency. Consequently, EC segments partially exhibit a rigid body motion with a displacement which is characterized by being in phase, of similar magnitude, and spatially in the same direction along all points on the EC wall within a segment. This phenomenon will be referred to as *nondeforming motions* of parts of the EC throughout this paper. Particularly, such a nondeforming motion of the EC parts at the EC entrance and TM causes the entrance plane and TM to change their positions in space, respectively, as a consequence of their connections with the surrounding structures. The motions of these boundaries complement the vibration of the EC wall, which has been widely accepted to primarily generate the sound pressure in the EC. The two cases of considering the motions of the EC entrance and TM due to nondeforming motion of adjacent EC parts and solely accounting for the vibration of the EC wall are illustrated in Fig. 1.

To the best of our knowledge, the effect of accounting for the motions of the EC entrance and TM due to nondeforming motion of the adjacent structures on the sound pressure in the open and occluded ear has not been quantified, yet. The objective of this paper is to study the impact of this phenomenon on the simulation of the OE, specifically focusing on effects related to the acoustic impedances at the EC

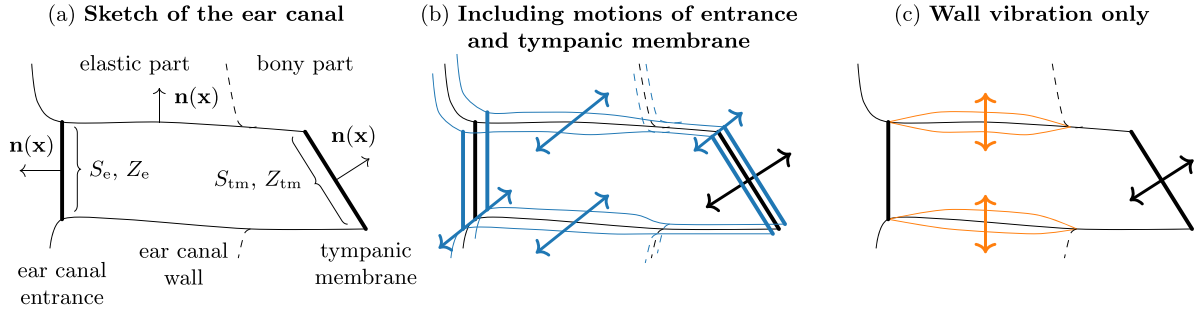

FIG. 1. (Color online) Sketch of the EC and its structural motion for BC stimulation. The dashed lines indicate the transition from the elastic part, consisting of cartilage and soft tissue, to the bony part. The EC entrance is depicted as a fictive plane. It is associated with a surface S_e and acoustic impedance Z_e, which represents an occluding device or the exterior radiation of sound in the case of the open ear, respectively. Likewise, the TM is associated with a surface S_{tm} and acoustic impedance Z_{tm}, incorporating the load by the middle and inner ear. $\mathbf{n}(\mathbf{x})$ denotes the unit vector perpendicular to the surfaces along positions $\mathbf{x}$. The colored lines and arrows illustrate the structural motion of the EC, the cause of the sound pressure in the EC, leading to a TM vibration (thick black arrows). In (b), an EC motion, including motions of the EC entrance and TM, are depicted, which are caused by nondeforming motion of the attached EC segments (blue double arrows). These motions complement the EC wall vibration. For comparison, an EC motion is illustrated in (c) (orange double arrows), where the TM vibration is solely due to the sound pressure generated by the wall vibration.

entrance and TM. Influencing factors and underlying mechanisms are discussed based on circuit calculations through examples using an EC motion extracted from a FE model of a human head.

II. MODELING CONSIDERATIONS

A. Formulation of the impedance boundary condition

Because the mechanism underlying the OE is the complex interaction of the vibrations of the EC structure with the sound field in the EC, OE models can be methodologically considered as fluid-structure problems (general information on fluid-structure problems can be found, e.g., in Ref. 37) Let Z be the acoustical impedance of a boundary attached to a moving structure (see Fig. 1), then the impedance boundary condition is[38,39]

$$v_a = p/Z + v_s\,, \quad \text{or } Z = \frac{p}{v_a - v_s}\,, \tag{1}$$

where p denotes the sound pressure, v_a is the normal acoustic particle velocity, and v_s is the associated velocity of the surrounding structure in normal direction to the boundary, which is often omitted.[39] Equation (1) states that v_s is to be superimposed on the reaction term p/Z to obtain the particle velocity, v_a, when solving a fluid-structure problem. From another perspective, it states that the *relative velocity*, $v_a - v_s$, between the air and its surrounding structure is to be incorporated to obtain the sound pressure, p.

Two examples highlight the validity of Eq. (1). For an acoustically rigid boundary ($Z \to \infty$), $v_a = v_s$, which means it moves with the adjacent solid. Neglecting v_s would misleadingly cause v_a to be zero in this case, implying that the acoustic boundary is fixed in position regardless of the surrounding structure's motion. If the structure is fixed ($v_s = 0$), Eq. (1) leads to the impedance definition $Z = p/v_a$, which is commonly used within OE models.

B. Application to OE models

As depicted in Fig. 1, the two boundaries often assigned with acoustic impedances for the simulation of the OE are the EC entrance and the TM (e.g., in Refs. 5, 6, 8, 13, 15, 18, and 20–22) The question is how to implement the impedance boundary condition from Eq. (1) into the simulation models to account for a nondeforming motion of the surrounding structures. Because it is a general phenomenon of structure-fluid interaction, it may affect both numerical approaches, e.g., using the FE method, and simplified approaches, such as equivalent circuit calculations. We begin the investigation by employing the circuit model depicted in Fig. 2 to provide a "visual image of the system."[40] It gives an overview of the physical mechanisms involved and allows separation of the various contributions to the TM sound pressure. Subsequently, an application of Eq. (1) to FE models is proposed.

1. Circuit modeling

In Fig. 2, the sound generation by the motion of the EC structure is divided into three volume velocity sources: $q_{w,s}$, $q_{e,s}$, and $q_{tm,s}$. Each of the sources corresponds to a specific boundary with distinct acoustic properties, necessitating their separate treatment. $q_{w,s}$ characterizes the volume velocity induced by the vibration of the EC wall,

$$q_{w,s} = -\int\!\!\int_{S_w} \mathbf{v_s}(\mathbf{x}) \cdot \mathbf{n}(\mathbf{x})\, \mathrm{d}S. \tag{2}$$

Here, S_w represents the surface of the EC wall, and $\mathbf{v_s}(\mathbf{x})$ is the complex-valued, three-dimensional structural velocity distribution along positions denoted as $\mathbf{x}$ on this surface. $\mathbf{n}(\mathbf{x})$ is the unit vector perpendicular to S_w at $\mathbf{x}$ in outward direction of the EC, as indicated in Fig. 1. Accordingly, the dot product $\mathbf{v_s}(\mathbf{x}) \cdot \mathbf{n}(\mathbf{x})$ captures the local normal component of the velocity. The negative sign in Eq. (2) accounts for the vector component to be defined outward while $q_{w,s}$ is, here, considered to be positive inward.

Note that Eq. (2) accounts for the vibration of the EC wall in general, which could include nondeforming motion of the parts. Yet, a nondeforming motion of an EC segment does not contribute to $q_{w,s}$. For such a motion, $\mathbf{v_s}$ remains constant across all positions on the wall within that segment. Consequently, the contributions of opposing boundaries within this segment to the overall volume velocity nullify each other as a result of the differing signs of $\mathbf{v_s}(\mathbf{x})\mathrm{d}\mathbf{S}(\mathbf{x})$. One should be aware that describing the EC wall vibration as source using the integral quantity $q_{w,s}$ is only valid as

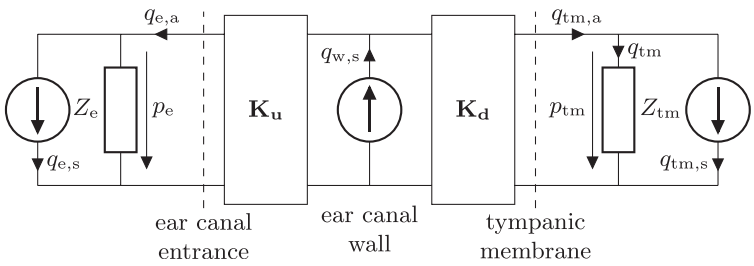

FIG. 2. Circuit model of the EC. The impedance Z_e represents an occluding device or the exterior radiation of sound in case of the open ear. Z_{tm} denotes the TM impedance. The motion associated with these boundaries because of their connections with the moving surrounding structures is considered with the sources $q_{e,s}$ and $q_{tm,s}$ parallel to Z_e and Z_{tm}. The vibration of the EC wall is represented by the volume velocity source $q_{w,s}$. It splits up the EC air volume into an upstream segment toward the EC entrance and a downstream segment terminated by the TM. For the circuit calculations presented here, the EC segments are modeled as acoustical transmission lines represented by two-port matrices $\mathbf{K_u}$ and $\mathbf{K_d}$.

https://doi.org/10.1121/10.0024244

long as the wavelength in air is much larger than the dimensions of the radiating wall area. This is the case, at least, in the considered frequency range below 1 kHz.

The source of strength $q_{e,s}$ represents the volume velocity corresponding to the motion with the surrounding structure of the EC entrance plane (see Fig. 1). The source in Fig. 2 is parallel to the impedance Z_e, which represents the occluding device (Z_e^{occl}), or the exterior radiation of sound out of the open ear (Z_e^{open}). The resulting equation regarding the acoustic volume velocity $q_{e,a}$ toward the EC entrance is

$$q_{e,a} = p_e/Z_e + q_{e,s}, \tag{3}$$

where p_e denotes the sound pressure at the EC entrance. Equation (3) is closely related to Eq. (1) but expressed with volume velocities instead of point velocities and with the impedance Z_e in Pas/m^3 based on the conception of a piston-like, one-dimensional motion of the boundary (see Sec. I). Note that $q_{e,s}$ refers to the passive motion of the EC entrance plane, which neglects the sound radiated into the EC from the outside, or the sound radiated by the occluding device (in that sense, the volume velocity imposed by the earplug as defined by Carillo *et al.*[22] represents both contributions). If desired, the radiation of an occluding device could be included by a second volume velocity source parallel to Z_e in the circuit in Fig. 2.

The volume velocity source $q_{tm,s}$ in Fig. 2 incorporates the motion of the TM caused by the nondeforming motion of the surrounding bone (see colored arrows in Fig. 1). $q_{tm,s}$ establishes the boundary condition

$$q_{tm,a} = p_{tm}/Z_{tm} + q_{tm,s}, \tag{4}$$

for the acoustical volume velocity $q_{tm,a}$ toward the TM, analogously to Eqs. (1) and (3). Here, p_{tm} denotes the sound pressure at the TM. Equation (4) states that the motion of the TM with the surrounding bone—represented by $q_{tm,s}$—is superimposed with the relative motion between ossicles and the surroundings due to the sound transmission from the TM to the inner ear, which is depicted by the term p_{tm}/Z_{tm}. Z_{tm} corresponds to the impedance that would be measured on human subjects using classical acoustical methods when there is no structural motion of the EC. Accordingly, it incorporates the complex deformation of the TM itself and the inertia of the ME ossicles (details on the TM impedance can be found, e.g., in Refs. 24–26, 28, 40, and 41) The formulation in Eq. (4) conceptually implies that the ME and inner ear structures move together with the TM and the surrounding temporal bone, therefore, BC sound transmitted from the ME into the EC via the TM (Refs. 7 and 20) is not accounted for. A second source could be added for this purpose if desired.

2. FE modeling

Equation (1) already gives the boundary condition for acoustic impedances within FE models, and a more detailed formulation is, e.g., given in Ref. 39. However, implementing Eq. (1) raises the question on how to obtain the structural velocity v_s.

Within such models, the TM is represented by its surface that is in contact with the air and assigned with the TM impedance rather than including it as a solid structure. In this case, a reasonable approach is to determine a vector $\bar{\mathbf{v}}_{\mathbf{tm,s}}$, as the component-wise average of the structural velocity over the mutual edge of the TM surface with the adjacent bone. The structural velocity, $v_{tm,s}$, which is included in the boundary condition, is then calculated locally as the normal component of $\bar{\mathbf{v}}_{\mathbf{tm,s}}$,

$$v_{tm,s}(\mathbf{x}) = \bar{\mathbf{v}}_{\mathbf{tm,s}} \cdot \mathbf{n}(\mathbf{x}). \tag{5}$$

Here, $\mathbf{n}(\mathbf{x})$ is the unit vector perpendicular to the TM surface at position $\mathbf{x}$ in outward direction of the EC (see Fig. 1). Including $v_{tm,s}$ in this manner in the acoustic boundary condition conceptually accounts for a piston-like motion of the TM surface, which follows the average structural motion of its edge. As already argued with regard to circuit models in Sec. II B 1, this formulation implies that the ME and inner ear structures align with this motion.

Obtaining the corresponding structural velocity $v_{e,s}$ at the EC entrance is feasible following the same approach by averaging via the mutual edge of the entrance plane with the surrounding structures. For instance, with a rigid impedance representing the occluding device, the resulting acoustic boundary condition in Eq. (1) locally accommodates the piston-like motion of the device with its surroundings. Thus, nonrigid devices and open-ear radiation just result in different impedance terms p / Z in Eq. (1), but the method for determining $v_{e,s}$ remains unchanged. However, it is essential to acknowledge that Eq. (1) solely accounts for sources inside the EC. To also encompass the BC-excited radiation from the head into the EC via the EC entrance,[19] an additional term would need to be incorporated.

The structural velocities in FE models and the volume velocities in the circuit approach are for the open and occluded ear cases related as

$$q_{e,s} = \int\int_{S_e} v_{e,s}(\mathbf{x})\,\mathrm{d}S, \quad q_{tm,s} = \int\int_{S_{tm}} v_{tm,s}(\mathbf{x})\,\mathrm{d}S. \tag{6}$$

Here, S_e and S_{tm} denote the surfaces of the entrance plane and TM as indicated in Fig. 1. Note that with the convention used here, $q_{e,s}$ is defined in outward direction normal to the entrance plane, and $q_{tm,s}$ is defined in direction toward the ME. The complex-valued relation of $q_{w,s}$, $q_{e,s}$, and $q_{tm,s}$ depends on the actual three-dimensional motion of the EC and orientation of the corresponding boundaries (see Sec. III B). Hence, a certain EC motion is implied implicitly or explicitly when conducting OE simulations. Given the relationship between the modeling approaches from Eq. (6), the circuit model from Fig. 2 is employed in the following to further elucidate the underlying mechanisms and discuss corresponding effects.

C. Effect on the simulation of the OE

To investigate the effect of the consideration of the structural EC motion within the impedance boundary conditions at EC entrance and TM, a formulation is now derived which explicitly reveals the dependency of the OE on the EC motion. This formulation is developed using the circuit model displayed in Fig. 2, where the EC motion finds representation through sources $q_{w,s}$, $q_{e,s}$, and $q_{tm,s}$. To accomplish this, the volume velocity $q_{tm} = q_{tm,a} - q_{tm,s}$ is scrutinized because it signifies the resulting *relative motion* between the TM and surrounding bone. It determines the TM pressure $p_{tm} = Z_{tm} q_{tm}$, which is transmitted through the ME to the inner ear, thereby representing the auditory perception in a manner analogous to air-conducted sound. Extending the approach of Ref. 6, volume velocity transfer functions T_w, T_e, and T_{tm} are defined to quantify the specific contributions of $q_{w,s}$, $q_{e,s}$ and $q_{tm,s}$ to q_{tm}, respectively, such that

$$q_{tm}^k = T_w^k q_{w,s}^k + T_e^k q_{e,s}^k + T_{tm}^k q_{tm,s}^k, \quad k \in \{\text{open}, \text{occl}\}. \tag{7}$$

The volume velocity transfer functions account for the observation that the induced volume velocities are divided into the branches in the circuit in Fig. 2 according to the impedance relations, therefore, only a part is transmitted to the TM. Consequently, as it is indicated in Eq. (7), their characteristics depend on whether the EC is open or occluded due to the corresponding impedance change at the EC entrance (see Ref. 6 for more details). The transfer functions may also encompass variations of the EC volume resulting from the insertion of an occluding device as indicated by the dependency on the occlusion condition in Eq. (7). This dependency is also denoted for $q_{w,s}$, $q_{e,s}$, and $q_{tm,s}$ to accommodate the factors outlined in Sec. I such as a variation of the radiating wall area[3,5] or the difference between the associated surfaces of the inserted occluding device and open EC entrance.

Using Eq. (7), the OE for a structural motion of the EC considering the vibration of the EC wall and the motions of the EC entrance plane and TM is

$$\begin{aligned} \text{OE} &= 20 \log_{10} \left| \frac{p_{tm}^{occl}}{p_{tm}^{open}} \right| \\ &= 20 \log_{10} \left| \frac{T_w^{occl} q_{w,s}^{occl} + T_e^{occl} q_{e,s}^{occl} + T_{tm}^{occl} q_{tm,s}^{occl}}{T_w^{open} q_{w,s}^{open} + T_e^{open} q_{e,s}^{open} + T_{tm}^{open} q_{tm,s}^{open}} \right|. \end{aligned} \tag{8}$$

Equation (8) expresses the OE directly as a function of the sources which represent the EC motion caused by BC stimulation. It highlights the two main influencing factors for the effect of the EC motion and its consideration at the TM and EC entrance on the OE: (1) the volume velocity transfer toward the TM, expressed by T_w, T_e, and T_{tm}; and (2) the relation and magnitudes of the different boundaries' motion, which are expressed by the volume velocities $q_{w,s}$, $q_{e,s}$, and $q_{tm,s}$. Accordingly, modeling assumptions regarding the EC motion—or the contributions of $q_{w,s}$, $q_{e,s}$, and $q_{tm,s}$—are, in principle, necessary for the simulation of the sound pressure at the TM and resulting OE.

However, the OE is commonly understood in a way that the vibration of the EC wall predominantly induces the sound pressure in the EC during the BC stimulation. This is a valid assumption when the magnitude of the wall's volume velocity, $|q_{w,s}|$, greatly surpasses the contributions of the EC entrance and TM, $|q_{e,s}|$ and $|q_{tm,s}|$ (see Fig. 1 for illustration). In this case, Eq. (8) simplifies to

$$\text{OE} \approx 20 \log_{10} \left| \frac{T_w^{occl} q_{w,s}^{occl}}{T_w^{open} q_{w,s}^{open}} \right|. \tag{9}$$

If it is additionally assumed that the fictive entrance plane of the open EC and surface of the occluding device are aligned (approximating a "shallow insertion" of an earplug) and the influence of the change in acoustical load caused by the occlusion on the vibration of the EC wall is negligible,[18] $q_{w,s}$ is then independent of the occlusion condition. Consequentially, the cancellation of $q_{w,s}$ in Eq. (9) results in an OE which depends only on the alteration of the volume velocity transfer function T_w.[6]

D. Circuit calculations for BC stimulation at the ipsilateral mastoid

We now demonstrate the effect of considering the EC wall vibration and the motions of the EC entrance and TM on the simulation of the OE using the circuit model in Fig. 2. The problem, however, is that each specific contribution of the boundaries involved depend on the type of excitation. As no general data on the spatially distributed motion of the EC for BC stimulation and the corresponding volume velocities are available yet, an example is taken as a case study.

The motions were extracted from the FE model of a human head presented by Xu *et al.*[19] The excitation was a BC stimulation of 1 N at the ipsilateral mastoid similar to a BC transducer.[5,12,13] The head base was fixed, and the tissue material properties denoted as "reference" in Ref. 19 were applied. Despite the adjustments at the EC entrance and TM described in Appendixes A and B, which serve the purpose of ensuring that the circuit calculations are representative in highlighting the mechanisms involved, the FE model was kept as documented in detail by Xu *et al.*[19] The volume velocities $q_{w,s}$, $q_{e,s}$, and $q_{tm,s}$, were extracted from the FE simulations following Eqs. (2) and (6) as reported in Appendix A. Subsequently, the volume velocity transfer functions were calculated based on the circuit in Fig. 2. Using the extracted volume velocities as input then allowed calculation of the terms $T_w q_{w,s}$, $T_e q_{e,s}$, and $T_{tm} q_{tm,s}$ from Eq. (7) as well as the resulting OE according to Eqs. (8) and (9).

To obtain the volume velocity transfer functions, the sound propagation within the EC needs to be considered. Therefore, the EC acoustics were modeled using a simplified circular cross section, cylindrical geometry with an EC length, l_{ec}, of 27.7 mm and radius, r_{ec}, to 3.85 mm. These dimensions lead to the same length and volume of the cylinder as those for the EC in the FE model.[19] The cylindrical geometry neglects the variability of the radius along the EC axis. The comparison between the circuit- and FE-calculated

https://doi.org/10.1121/10.0024244

sound pressure in Appendix B shows that the circuit calculations can be considered to appropriately represent the mechanisms related to the motions of the EC entrance plane and TM.

As indicated in Fig. 2, the motion of the EC wall is represented by a point source with the volume velocity $q_{w,s}$ splitting up the EC air volume into an upstream segment toward the EC entrance and a downstream segment terminated by the TM.[6,8,15,20] The EC segments were modeled as lossless acoustical transmission lines represented by two-port matrices, $\mathbf{K_u}$ and $\mathbf{K_d}$.[15,42] The entries in $\mathbf{K_u}$ were obtained as[42]

$$\mathbf{K_u} = \begin{pmatrix} \cos kl_u & jZ_0 \sin kl_u \\ \frac{j}{Z_0} \sin kl_u & \cos kl_u \end{pmatrix}, \tag{10}$$

with wavenumber $k = 2\pi f/c_0$, characteristic impedance $Z_0 = \rho_0 c_0/(\pi r_{ec}^2)$, the speed of sound in air $c_0 = 343$ m/s, and the density of air $\rho_0 = 1.2$ kHz. The length of the upstream and downstream segments, l_u and l_d, were set to 8 mm and 19.7 mm, respectively, which lead to an appropriate agreement of the circuit-calculated TM pressure with corresponding FE results (see Appendix B). $\mathbf{K_d}$ was calculated according to Eq. (10) with l_d instead of l_u. It is worth noting that using lossless transmission lines to model the EC acoustics assumes that the air's inertia or compliance effect are dominant compared to the viscous and thermal losses. Carillo *et al.*[8] showed that these losses do not significantly influence the sound pressure and volume velocity flow in the EC within the considered frequency range. The volume velocity transfer in direction to the wall due to its vibration is accounted for by $q_{w,s}$ according to Eq. (2).

At the TM, the impedance, Z_{tm}, was taken from Shaw and Stinson.[23] It was implemented according to the values given in Ref. 20. Z_{tm} exhibits a resonance at about 900 Hz, and below it acts as a compliance. Two occlusion conditions were considered at the EC entrance. For the first condition, a perfect occlusion was modeled by setting Z_e^{occl} to infinity. The second occluding condition represents a vented earplug with a hole of 0.9 mm radius and 21 mm length. This condition was already used for the circuit calculations by Carillo *et al.*[6] for comparison with experimental data by Hansen[15] (here called "vented" condition is termed "partially occluded" in Ref. 6). The air in the vent, the air in the EC, and the TM compliance form a Helmholtz resonator with a resonance frequency of about 400 Hz.[6] For the corresponding calculations, the same volume velocities $q_{w,s}^{occl}$, $q_{e,s}^{occl}$, and $q_{tm,s}^{occl}$, as employed for the perfectly occluded case were used.

The radiation impedance, Z_e^{open}, at the EC entrance for the open ear was obtained from the FE model by an accompanying simulation with a piston-like excitation at the entrance plane toward the exterior of the head. For this simulation, the "perfectly matched layer," which allows a free field radiation without reflection, was used as described in Ref. 19, and the head surfaces were modeled as acoustically rigid. Z_e^{open} is inertia dominated within the inspected frequency range.

III. RESULTS

In Fig. 3, the OE calculations according to Sec. II D for an EC motion, which accounts for the vibration of the EC wall and the motions of the EC entrance and TM, and when only considering the EC wall contribution are shown for a perfectly occluded (left) and vented EC (right). To illustrate the influence on the sound pressure at the TM itself, the level differences between the calculations of the sound pressure, including both mechanisms and exclusively accounting for the wall vibration, are displayed in Fig. 4. These were computed from the ratio $q_{tm}/(T_w q_{w,s})$ for the open (left), perfectly occluded (center), and vented (right) EC entrance conditions. In Fig. 5, the relative contributions $T_w q_{w,s}$ (orange), $T_e q_{e,s}$ (green), and $T_{tm} q_{tm,s}$ (purple) are shown normalized to their resulting sum, q_{tm} [see Eq. (7)]. These curves represent the contributions of the motion associated with the wall, the EC entrance, and TM to the sound pressure at the TM.

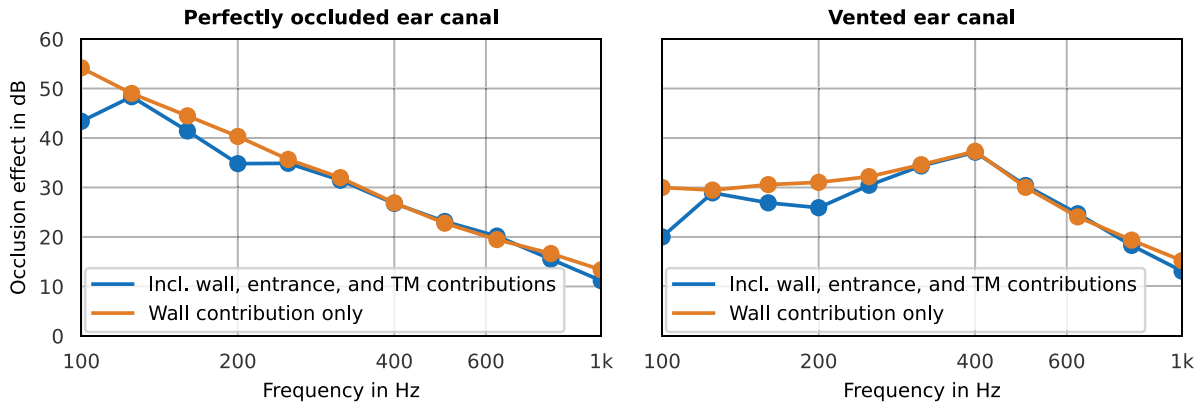

FIG. 3. (Color online) OE calculations for an EC motion, including the vibration of the EC wall and the motions of the EC entrance and TM according to Eq. (8) (blue) and the OE calculated solely from the vibration of the EC wall according to Eq. (9) (orange). The OE is computed based on third octave band averages and given for the perfectly occluded and vented EC entrance. These calculations highlight the role of the EC motion for two occlusion conditions (left and right). In contrast to the OE calculated solely based on the EC wall's contribution, accounting for the motions of the EC entrance and TM leads to a reduction of the OE in the lowest frequency range. However, the two curves align toward 1 kHz.

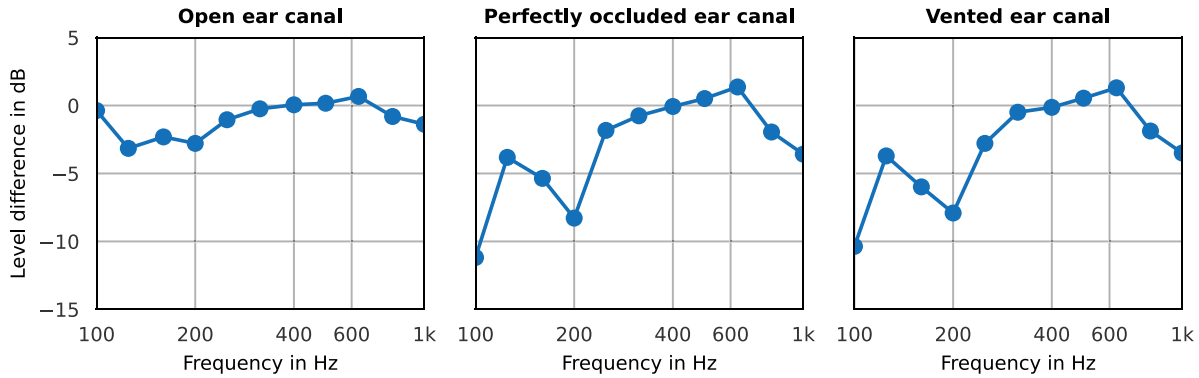

FIG. 4. (Color online) TM sound pressure level difference between the calculation for an EC motion, which accounts for the vibration of the EC wall and the motions of the EC entrance and TM, and the calculation exclusively considering wall's contribution. The level difference is computed from third octave band averages and provided for the open, perfectly occluded and vented EC entrance conditions. These calculations highlight the influence of the motions of the EC entrance and TM on the sound pressure at the TM. In contrast to sound pressure calculated ignoring these contributions, a reduction in sound pressure is observed in the lowest frequency range. However, this reduction is more pronounced in the occluded conditions compared to the open ear.

The narrowband data extracted from the FE simulations exhibit strong resonances, especially at the lowest frequencies below 300 Hz (see Fig. 6 in Appendix A). To better illustrate the general trends, the results were calculated from third octave band averages of the overall volume velocities, $q_{\mathrm{tm}}^{\mathrm{open}}$ and $q_{\mathrm{tm}}^{\mathrm{occl}}$, in Fig. 3 [the numerator and denominator in Eq. (8)] and the contributors $T_{\mathrm{w}}q_{\mathrm{w,s}}$, $T_{\mathrm{e}}q_{\mathrm{e,s}}$, and $T_{\mathrm{tm}}q_{\mathrm{tm,s}}$, as well as their sum, q_{tm}, in Figs. 4 and 5. The center frequencies were chosen according to the IEC 61260-1:2014 standard.[46]

A. Wall vibration only

The results for the OE only based on the vibration of the EC wall depicted in Fig. 3 (orange lines) were calculated according to Eq. (9). The curves resemble the results in Ref. 6 (Fig. 5) with the small distinction that, here, the difference between the volume velocities $q_{\mathrm{w,s}}^{\mathrm{open}}$ and $q_{\mathrm{w,s}}^{\mathrm{occl}}$, which was below 2 dB throughout the whole frequency range of interest, is accounted for. The related mechanisms are briefly summarized in the following. This will help to understand the additional effects when the contributions of the EC entrance and TM are accounted for in Sec. III B.

For the perfectly occluded EC entrance (left), the OE exhibits the well-known second order low-pass filter characteristic.[6] It can be explained by the variation of the volume velocity transfer from the wall toward the TM, which determines the OE according to Eq. (9) for the case of $q_{\mathrm{w,s}}^{\mathrm{open}} \approx q_{\mathrm{w,s}}^{\mathrm{occl}}$ given here. In the open case, the wall's volume velocity is mainly transferred toward the EC entrance as a result of the low impedance of the inertia of the air in the upstream section and the EC entrance. With increasing frequency, this transfer is reduced because of the increase in the inertial impedance and the decreasing impedance of the TM and downstream air compliance. In the occluded case, the transfer of the volume velocity toward the TM is constant with frequency caused by the pressure chamber effect of the compliant EC volume, resulting in the low-pass characteristic of the OE.[6]

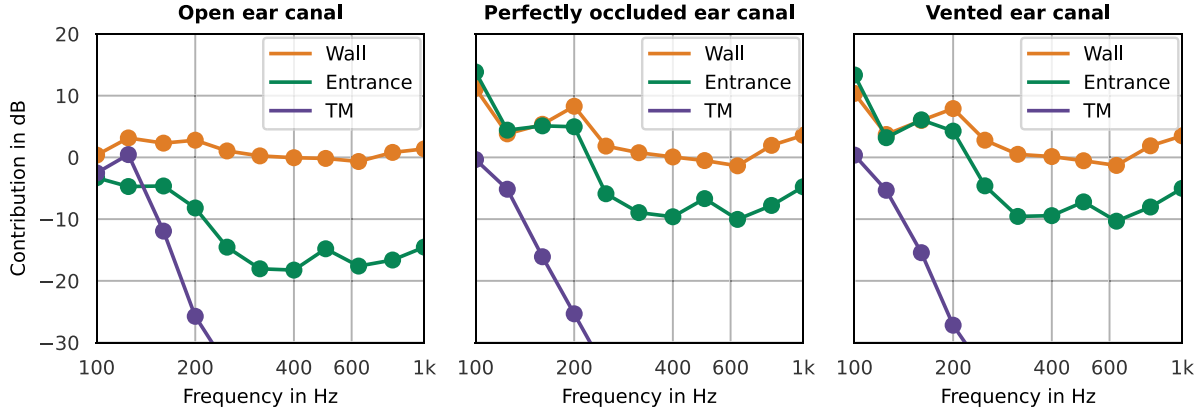

FIG. 5. (Color online) Volume velocity contributions associated with the EC boundaries to the TM sound pressure. Following Eq. (7), the three terms $T_{\mathrm{w}}q_{\mathrm{w,s}}$ (orange), $T_{\mathrm{e}}q_{\mathrm{e,s}}$ (green), and $T_{\mathrm{tm}}q_{\mathrm{tm,s}}$ (purple) normalized to their sum q_{tm} for the open (left), perfectly occluded (center), and vented EC (right) scenarios are illustrated. These ratios are based on third octave band averages. In the open-ear case (left), the wall's contribution dominates across the entire frequency range. Conversely, in the two occluding scenarios, the wall and entrance contributions exhibit similar magnitudes at the lowest frequencies. Notably, both contributions maintain magnitudes exceeding 0 dB within this frequency range, indicating a partial cancellation effect. This cancellation leads to a reduction in the TM sound pressure when compared to scenarios where only the wall's contribution is considered.

https://doi.org/10.1121/10.0024244

The vent at the EC entrance causes a reduction of the OE compared to the perfect occlusion because it allows for a volume velocity transfer from the EC wall through the vent instead of toward the TM below the Helmholtz resonance (cf. right panel in Fig. 3).[6] The OE is constant with frequency within this frequency range. Above the resonance, the air in the vent occludes the EC entrance, hence, the OE for vented EC entrance and the case of perfect occlusion follow a similar trend.

B. Including contributions of the entrance plane and TM

The OE results in Fig. 3 (blue lines) represent an illustrative example considering the wall vibration and the motions of the EC entrance plane and TM. In contrast to the prevalent assumption in OE simulations, which predominantly considers wall vibration alone (orange lines), the OE is reduced in the 100, 160, and 200 Hz third octave bands while the curves are similar at other frequencies. This OE reduction can, in principle, be attributed to changes in the open or occluded ear sound pressure. Therefore, Fig. 4 shows the effect of the contributions of the EC entrance and TM to the TM sound pressure itself, examined for the scenarios with open EC (left), perfectly occluded EC (center), and vented EC (right). In contrast to sound pressure calculated solely from the vibration of the EC wall, a reduction is observed in the lowest frequency range. However, this reduction is more pronounced in the occluded conditions compared to the open ear, which results in the reduction of the OE displayed in Fig. 3.

Figure 5 helps to identify the underlying mechanisms which explain the difference of the effect between the open and occluding conditions on the TM sound pressure and shows the relative contributions of the three distinct volume velocities associated with the wall (depicted in orange), the EC entrance (green), and TM (purple) to the resulting sound pressure at the TM. In the case of the open ear, the wall's contribution predominantly influences the TM pressure above 250 Hz (as shown in the left plot of Fig. 5) as it closely approaches 0 dB. In the 125, 160, and 200 Hz third octave bands, the wall's contribution exhibits a magnitude slightly greater than 0 dB, which indicates a partial cancellation by the TM's contribution at 125 Hz and by the entrance's contribution at 160 and 200 Hz. Interestingly, the entrance's and TM's contributions cancel each other at 100 Hz, resulting in the wall's contribution to be dominant. Consequently, the difference in Fig. 4 (left panel) is relatively small except between 125 and 200 Hz, where accounting for motion of EC entrance and TM reduces the TM sound pressure by approximately 3 dB.

For the perfectly occluded and vented conditions, the wall's contribution predominates only for frequencies higher than approximately 250 Hz (right and center plots in Fig. 5). Below 250 Hz, the entrance's and the wall's contributions are similar in magnitude. What is noteworthy here is that both contributions exhibit a magnitude greater than 0 dB, signifying their partial cancellation in this frequency range. Conceptually, this can be visualized as the rigid EC entrance plane moving together with the attached wall but with different surface orientations. This type of motion leads to an overall reduction of the volume velocity when these contributions are summed [see also explanations on Eq. (2)]. Consequentially, the occluded TM pressure is reduced. This phenomenon is very similar for the two cases of perfect occlusion and a vented EC entrance considered here. Accordingly, when only accounting for the wall's contribution for the OE (orange line in Fig. 3), this effect, stemming from the reduction of the wall's contribution resulting from the motion of the entrance plane, is omitted. This omission leads to an overestimation of the predicted occluded sound pressure.

Notably, in all three cases, the contribution linked to the motion of the TM with the surrounding bone remains small, except at the lowest considered frequencies below 125 Hz (purple lines in Fig. 5). This phenomenon can be attributed to the different materials surrounding the EC. At the lowest frequencies inspected, the EC exhibits a rigid body motion as a whole. However, already above approximately 125 Hz, the EC section surrounded by soft tissue and cartilage exhibits a higher amplitude of the motion than the bony part attached to the TM. Consequently, the resulting volume velocity associated with the TM remains significantly smaller in magnitude when compared to the volume velocities linked to the wall and EC entrance plane. The only exception is the 125 Hz band with open ear, where the volume velocity associated with the motion of the TM partially cancels the effect of the wall vibration on the TM pressure.

Another illustration of the mechanisms is provided with the help of the circuit in Fig. 2. The three sources are connected to two branches each with one portion of the volume velocity flowing toward the TM—encompassed by the volume velocity transfer functions—and another portion directed toward the EC entrance. The high impedance at the EC entrance for the two occluding conditions causes the portion toward the EC entrance to be relatively small. This leads to $|T_{\mathrm{w}}^{\mathrm{occl}}| \approx |T_{\mathrm{e}}^{\mathrm{occl}}| \approx |T_{\mathrm{tm}}^{\mathrm{occl}}|$, allowing the partial cancellation of the wall's contribution by the entrance's contribution below 250 Hz, because of their phase differences related to the surface orientations. In contrast, for the open-ear condition, the air in the EC is divided into an upstream and a downstream section[6,8,15,20] connected to the low radiation impedance at the EC entrance. This division results in different ratios of the volume velocity portions transmitted toward the EC entrance and TM for each of the sources. Most significantly, it leads to $|T_{\mathrm{e}}^{\mathrm{open}}| < |T_{\mathrm{w}}^{\mathrm{open}}|$. Consequently, the effect of the entrance's contribution to cancel the wall's contribution is smaller for the open compared to the occluded conditions, as shown when comparing the green lines in Fig. 5.

IV. DISCUSSION

A. Comparison to experimental findings

The differences for the perfectly occluded and vented EC entrance highlight that the magnitude and filter characteristic of the OE potentially varies depending on the EC

motion. Especially, the considered example indicates that a reduction of the OE toward the lowest frequencies compared to the second order low-pass filter characteristic[6] can be related to nondeforming motion of parts of the EC (cf. Fig. 3)—which was not accounted for at the EC entrance and TM in previous studies of the topic. Indeed, comparisons between experimental data obtained from EC sound pressure measurements and OE simulations[18,19,22] reveal an overestimation of the OE, in particular, at frequencies below 250 Hz.

Reinfeldt *et al.*[12] found a higher variance of the OE obtained from EC sound pressure measurements for ipsilateral mastoid stimulation with a BC transducer at lowest frequencies compared to other positions on the skull and stated that this could be related to the elastic part of the EC being closer to the ipsilateral position. Saint-Gaudens *et al.*[16] reported the same effect comparing ipsi- and contralateral stimulation, whereas the variance was comparable with mastication as BC stimulation. The OE calculation with stimulation at the mastoid reveals the influence in the same frequency range where the higher variance is observed in the measurements. It is likely that the numerous factors listed in Sec. III B result in variations of the EC motion. Accordingly, it is plausible that the mechanisms considered within this study, which are related to the EC motion, contribute to the observed variance of the open or occluded sound pressure (cf. Fig. 4) and the OE (cf. Fig. 3).

B. Simulation of the OE

Figure 3 highlights the effect of considering the motions of the EC entrance and TM on the OE simulation. Accordingly, additional parameters $q_{e,s}$ and $q_{tm,s}$ [cf. Eq. (8)] could improve the prediction of the sound pressure in the EC and OE with circuit models. However, the values of $q_{w,s}$, $q_{e,s}$, and $q_{tm,s}$ depend on the EC geometry, the orientation and magnitude of the excitation, the areas associated with the volume velocity sources, and the material properties of the EC surroundings. More experimental and numerical studies are needed to investigate the EC motion in more detail in the future, e.g., in terms of the spatially distributed EC wall vibration (as already pointed out by Carillo *et al.*[22]) This is also indicated by a remaining difference of the open-ear pressure between the FE simulation and circuit calculation given in Fig. 7 in Appendix B. This difference can potentially be mitigated by considering the frequency-dependent nature of the velocity distribution, particularly in terms of its centroid position.[22] For the circuit calculations conducted within this study, a constant centroid position with frequency was assumed.

Within numerical models, one should be aware that applying the TM impedance locally as specific acoustic impedance deviates from the original one-dimensional formulation (see, e.g., detailed discussion in Ref. 24). Also, the pressure distribution in the EC (especially close to the TM)[31,43] and the deformation of the TM is generally complex at higher frequencies than about 1–1.5 kHz.[29,30] Therefore, it is reasonable to replace the impedances at the EC entrance and the TM, e.g., considering the coupling of the EC cavity with the external air,[19] or using middle and inner ear structures at the TM.[44] Although this allows extending the frequency range of the OE simulations, it increases the model complexity and computational effort. Yet, circuit and FE models have been shown to be useful to investigate the OE using acoustic impedances (see, e.g., Ref. 8 for a comparison). The proposed extension of the impedance boundary condition could help to improve such OE simulations by accounting for nondeforming motion of the EC.

C. Mechanisms contributing to the OE

Within the FE simulations and circuit calculations conducted for this study, an impedance was applied at the EC entrance plane instead of including the earplug as solid material. Thereby, the effects of occluding devices listed in Sec. I, which are not directly related to its impedance, such as the variation of the radiating area,[3,5] were excluded. Although this is a limitation of the study regarding the prediction of the occluded sound pressure in the EC, it allowed focusing on the consideration of the motion of the earplug's medial surface due to its connection with the surroundings throughout the analysis. Similarly, also the open EC entrance was only considered using a radiation impedance. However, Xu *et al.*[19] compared OE simulations with the same FE model of a human head as employed here between a setup with a radiation impedance at the EC entrance and an infinite surrounding acoustic domain directly coupled to the EC cavity (see their Fig. 8). Additional simulations with incorporating the impedance boundary condition according to Eq. (1) confirmed their finding that the sound radiation of the head vibrations into the open EC via the EC entrance can contribute to TM sound pressure, especially at the lowest frequencies (refer to Appendix C for more details).[19]

Accordingly, the present considerations highlight that at least three influencing factors, namely (a) vents of the occluding device or leaks at the EC entrance, (b) the radiation of BC-stimulated sound into the open EC, and (c) the nondeforming motion of parts of the EC, contribute to the deviation of the OE from a second order low-pass filter characteristic. Comparable mechanisms, which could additionally influence the TM sound pressure, are the radiation of sound by the earplug[22] and BC sound transmitted through the ME into the EC.[7] These effects associated with the EC entrance and TM were excluded here in favor of only investigating the role of the structural motion of the EC. Yet, the considered example indicates the necessity to distinguish between the various mechanisms. However, it remains challenging to predict their effect on the resulting EC sound pressure and OE in advance because these mechanisms contribute to the TM pressure differently depending on whether the EC is open or occluded (as exemplified in Fig. 5). Also, the present analysis considered the EC motion only in a specific head model for a particular BC stimulation at the

https://doi.org/10.1121/10.0024244

mastoid. The variability of the aforementioned mechanisms in relation to the factors listed in Sec. I, such as the type of stimulation or the individual EC geometry, remains unexplored. A more comprehensive investigation into these complexities could be a valuable pursuit for future research.

V. CONCLUSION

This study highlighted the impact of a nondeforming motion of parts of the EC on the sound pressure at the TM and the resulting OE. This type of motion causes the EC entrance and the TM to move with their surrounding structures. As a result, these boundaries' contributions complement the vibration of the EC wall in serving as the source of the BC-stimulated sound pressure in the EC, particularly at the lowest frequencies. An impedance boundary condition was proposed, which incorporates this phenomenon by including a term to consider the structural motion of the adjacent solids at EC entrance and TM. When applied to OE models, the effect of this motion depends on two key factors: first, the volume velocity transfer from the boundaries represented by acoustic impedances to the TM, which varies based on the open or occluded condition at the EC entrance and, second, the frequency-dependent, three-dimensional motion of the EC itself. To illustrate the related mechanisms, an example motion with BC stimulation at the mastoid was extracted from a FE model of a human head. This motion was employed as input for circuit calculations, considering perfectly occluded and vented EC scenarios.

The results revealed that the motions of the EC entrance and TM caused by nondeforming adjacent EC parts—which is addressed by the proposed extension—can contribute to a reduction of the TM sound pressure at the lowest frequencies compared to when solely accounting for the vibration of the EC wall. This impact was found to be more pronounced when the EC is occluded, leading to a concurrent reduction of the OE. It is reasonable to consider that the mechanisms associated with the motions of the occluding device and TM offer a plausible explanation of the higher variance of experimental OE data for stimulation positions close to the EC. In addition, they can contribute to the deviation between OE simulations and experimental data below 250 Hz.

The considered EC motion highlighted the importance of discerning between multiple mechanisms that contribute to the sound pressure at the TM in open or occluded scenarios. Yet, a more detailed knowledge on the EC motion and its influencing factors is needed to determine the relative contributions of the various effects and their degree of variability before, e.g., including the contributions by the different surfaces within improved circuit simulations of the OE.

SUPPLEMENTARY MATERIAL

See the supplementary material for a Python script (Python Software Foundation)[45] with the circuit calculations, and the corresponding data extracted from the FE simulations.

ACKNOWLEDGMENTS

The authors would like to thank Steffen Marburg for pointing to the literature to base the considerations on. This work was funded by the Deutsche Forschungsgemeinschaft (DFG, German Research Foundation)—Project-ID 352015383—SFB 1330 A4 and supported through a Mitacs Globalink Research Award (Ref. No. IT34758).

AUTHOR DECLARATIONS

Conflict of Interest

All authors have no conflicts to disclose.

DATA AVAILABILITY

The data that support the findings of this study are available within the article and its supplementary material.

APPENDIX A: FE SIMULATIONS

Open and perfectly occluded conditions were applied at the EC entrance in the FE model (at the position termed "E1" in Ref. 19) using the same impedances as were used for the circuit calculations. Likewise, the TM impedance after Shaw and Stinson[20,23] was used at the TM. The circuit impedances (in Pas/m^3) were multiplied with the area of the corresponding boundary surfaces to apply them locally as specific acoustic impedances (in Pas/m). To account for the

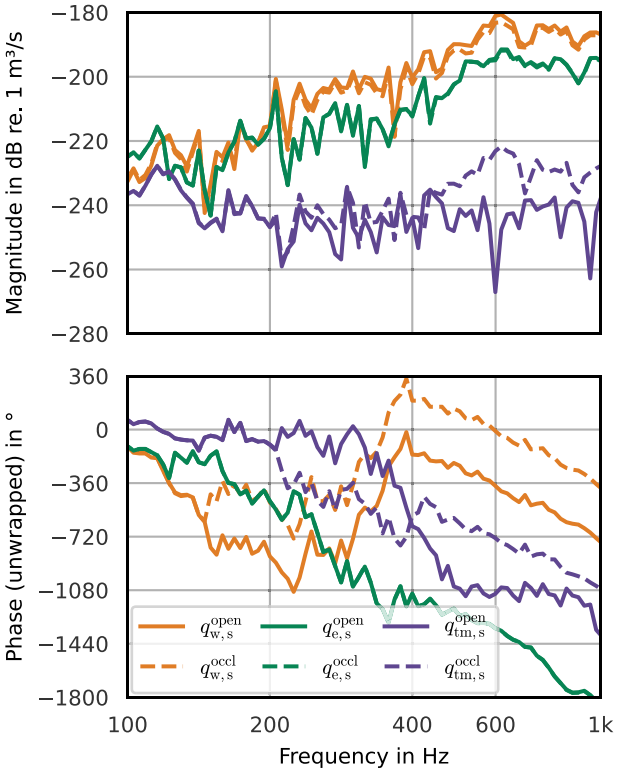

FIG. 6. (Color online) Magnitude and unwrapped phase of the volume velocities extracted from the FE simulations for BC stimulation of 1 N at the ipsilateral mastoid (right ear).

structural motion at the boundaries represented by acoustic impedances, the underlying equations in the software COMSOL Multiphysics® version 6.1 (COMSOL AB, Stockholm, Sweden), which was used for the FE simulations, were manually modified as described in Sec. II B 2. Given these simulation parameters, the volume velocities $q_{w,s}^{open}$ and $q_{w,s}^{occl}$ were extracted according to Eq. (2), and $q_{e,s}^{open}$, $q_{e,s}^{occl}$, $q_{tm,s}^{open}$, and $q_{tm,s}^{occl}$ were obtained according to Eq. (6). The volume velocities are depicted in Fig. 6. The inspected frequency range included the third octave bands from 100 Hz to 1 kHz. The frequency resolution was set to 24 frequencies per octave.

APPENDIX B: VALIDATION OF CIRCUIT CALCULATIONS

To ensure that the circuit calculations are representative in highlighting the mechanisms involved, the calculations were verified by simulating the TM pressure for the open-ear condition with radiation impedance and perfectly occluded condition with infinite impedance at the EC entrance. The comparison is displayed in Fig. 7.

The sound pressure level difference between the FE simulation and circuit calculation with perfectly occluded EC is generally negligible within the examined frequency range. The level difference for the open EC is relatively small except in the 200 Hz third octave band, where the circuit-calculated sound pressure is about 6 dB higher than that in the FE simulation. This difference can be potentially attributed to the assumption of a constant length for the EC segments (8 and 19.7 mm) across all frequencies. This is a

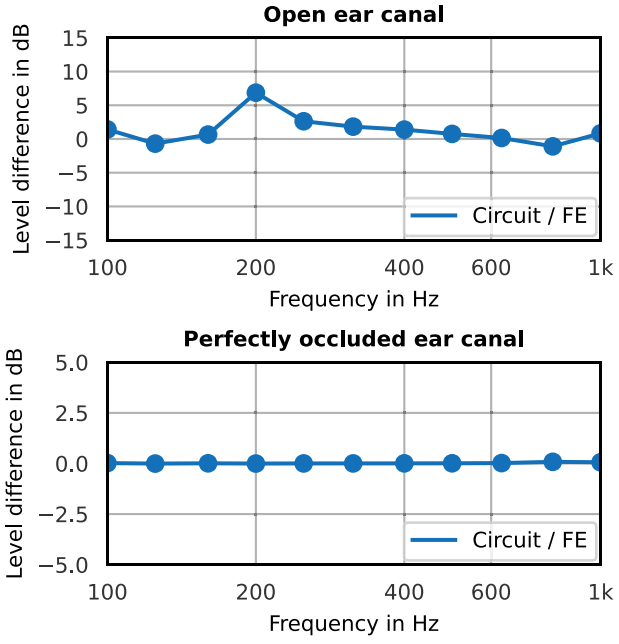

FIG. 7. (Color online) Comparison between the TM sound pressure from the circuit calculations and the FE simulations for the open and perfectly occluded impedance conditions at the EC entrance. The level difference between circuit calculation and FE simulation is calculated from third octave band averages.

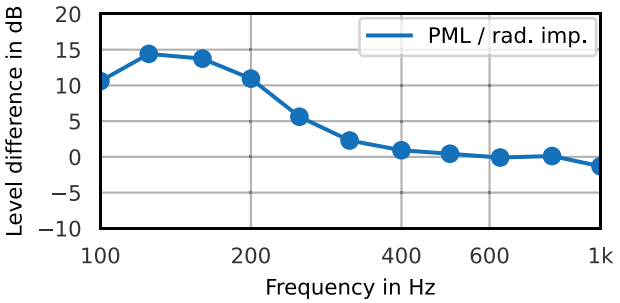

FIG. 8. (Color online) Comparison between the TM sound pressure from the FE simulations with radiation impedance conditions (rad. imp.) at the EC entrance and a perfectly match layer (PML) around the head following Xu *et al.* (Ref. 19). The level difference is calculated from the third octave band averages.

simplification of the potentially frequency-dependent effect where the air in the EC is split up into an inertia-dominated part toward the EC entrance and a compliant section toward the TM.[6] However, it is crucial to note that this simplification does not compromise the fundamental findings regarding the impact of the motions of the EC entrance plane and TM on TM sound pressure. This is best illustrated by the negligible difference visible between circuit calculation and FE simulation for the perfectly occluded EC in Fig. 7, whereas the effects of the different contributors to the TM sound pressure are most pronounced in this case (see Fig. 4, center plot). Therefore, the circuit calculations can be considered to appropriately represent the relevant mechanisms involved.

APPENDIX C: RADIATION INTO THE OPEN EC

In addition to the radiation impedance at the EC entrance, a FE simulation with a perfectly matched layer around the head was conducted in the same way as the corresponding setup by Xu *et al.*,[19] but including the impedance boundary condition at the TM according to Sec. II B 2. Compared to the radiation impedance at the EC entrance, this simulation condition also accounts for the exterior radiation of the BC-stimulated head vibrations into the EC. The difference between the resulting TM pressure simulations is shown in Fig. 8. Accordingly, the main effect of the sound propagation from the exterior into the EC is an increase in the TM sound pressure below approximately 300 Hz. This effect further reduces the resulting OE compared to Fig. 3. Note that this contribution to the TM sound pressure in the open ear is not represented within the circuit model used for the present study.

[1]E. H. Berger and J. E. Kerivan, "Influence of physiological noise and the occlusion effect on the measurement of real-ear attenuation at threshold," J. Acoust. Soc. Am. **74**(1), 81–94 (1983).
[2]O. Doutres, F. Sgard, J. Terroir, N. Perrin, C. Jolly, C. Gauvin, and A. Negrini, "A critical review of the literature on comfort of hearing protection devices: Definition of comfort and identification of its main attributes for earplug types," Int. J. Audiol. **58**(12), 824–833 (2019).
[3]H. Dillon, "Venting and the occlusion effect," in *Hearing Aids*, 2nd ed. (Boomerang, Sydney, 2012), pp. 140–144.

[4]J. Tonndorf, "A new concept of bone conduction," Arch. Otolaryngol. **87**(6), 595–600 (1968).
[5]S. Stenfelt and S. Reinfeldt, "A model of the occlusion effect with bone-conducted stimulation," Int. J. Audiol. **46**(10), 595–608 (2007).
[6]K. Carillo, O. Doutres, and F. Sgard, "On the removal of the open earcanal high-pass filter effect due to its occlusion: A bone-conduction occlusion effect theory," Acta Acust. **5**, 36 (2021).
[7]S. Stenfelt, T. Wild, N. Hato, and R. L. Goode, "Factors contributing to bone conduction: The outer ear," J. Acoust. Soc. Am. **113**(2), 902–913 (2003).
[8]K. Carillo, O. Doutres, and F. Sgard, "Theoretical investigation of the low frequency fundamental mechanism of the objective occlusion effect induced by bone-conducted stimulation," J. Acoust. Soc. Am. **147**(5), 3476–3489 (2020).
[9]K. Carillo, O. Doutres, and F. Sgard, "Principle of an acoustical method for estimating the centroid position of the earcanal wall normal velocity induced by bone-conducted stimulation: Numerical evaluation," Appl. Acoust. **182**, 108245 (2021).
[10]M. R. Stinson and B. W. Lawton, "Specification of the geometry of the human ear canal for the prediction of sound-pressure level distribution," J. Acoust. Soc. Am. **85**(6), 2492–2503 (1989).
[11]A. P. Balouch, K. Bekhazi, H. E. Durkee, R. M. Farrar, M. Sok, D. H. Keefe, A. K. Remenschneider, N. J. Horton, and S. E. Voss, "Measurements of ear-canal geometry from high-resolution CT scans of human adult ears," Hear. Res. **434**, 108782 (2023).
[12]S. Reinfeldt, S. Stenfelt, and B. Håkansson, "Estimation of bone conduction skull transmission by hearing thresholds and ear-canal sound pressure," Hear. Res. **299**, 19–28 (2013).
[13]M. K. Brummund, F. Sgard, Y. Petit, F. Laville, and H. Nélisse, "An axisymmetric finite element model to study the earplug contribution to the bone conduction occlusion effect," Acta Acust. Acust. **101**(4), 775–788 (2015).
[14]J. Wang, S. Stenfelt, S. Wu, Z. Yan, J. Sang, C. Zheng, and X. Li, "The effect of stimulation position and ear canal occlusion on perception of bone conducted sound," Trends Hear. **26**, 1–15 (2022).
[15]M. Ø. Hansen, "Occlusion effects, part II: A study of the occlusion effect mechanism and the influence of the earmould properties," Ph.D. dissertation, Technical University of Denmark, Lyngby, Denmark, 1998.
[16]H. Saint-Gaudens, H. Nélisse, F. Sgard, and O. Doutres, "Towards a practical methodology for assessment of the objective occlusion effect induced by earplugs," J. Acoust. Soc. Am. **151**(6), 4086–4100 (2022).
[17]F. Denk, T. Hieke, M. Roberz, and H. Husstedt, "Occlusion and coupling effects with different earmold designs—All a matter of opening the ear canal?," Int. J. Audiol. **62**, 227 (2022).
[18]M. K. Brummund, F. Sgard, Y. Petit, and F. Laville, "Three-dimensional finite element modeling of the human external ear: Simulation study of the bone conduction occlusion effect," J. Acoust. Soc. Am. **135**(3), 1433–1444 (2014).
[19]H. Xu, F. Sgard, K. Carillo, É. Wagnac, and J. de Guise, "Simulation of the objective occlusion effect induced by bone-conducted stimulation using a three-dimensional finite-element model of a human head," J. Acoust. Soc. Am. **150**(5), 4018–4030 (2021).
[20]J. Schroeter and C. Poesselt, "The use of acoustical test fixtures for the measurement of hearing protector attenuation. Part II: Modeling the external ear, simulating bone conduction, and comparing test fixture and real-ear data," J. Acoust. Soc. Am. **80**(2), 505–527 (1986).
[21]T. Zurbrügg, A. Stirnemannn, M. Kuster, and H. Lissek, "Investigations on the physical factors influencing the ear canal occlusion effect caused by hearing aids," Acta Acust. Acust. **100**(3), 527–536 (2014).
[22]K. Carillo, O. Doutres, and F. Sgard, "Numerical investigation of the earplug contribution to the low-frequency objective occlusion effect induced by bone-conducted stimulation," J. Acoust. Soc. Am. **150**(3), 2006–2023 (2021).
[23]E. A. G. Shaw and M. R. Stinson, "The human external and middle ear: Models and concepts," in *Mechanics of Hearing*, edited by E. de Boer and M. A. Viergever (Springer, Dordrecht, Netherlands, 1983), pp. 3–10.
[24]H. Hudde and A. Engel, "Measuring and modeling basic properties of the human middle ear and ear canal. Part I: Model structure and measuring techniques," Acta Acust. Acust. **84**(4), 720–738 (1998), available at https://www.ingentaconnect.com/content/dav/aaua/1998/00000084/00000004/art00016.
[25]H. Hudde and A. Engel, "Measuring and modeling basic properties of the human middle ear and ear canal. Part II: Ear canal, middle ear cavities, eardrum, and ossicles," Acta Acust. Acust. **84**(5), 894–913 (1998), available at https://www.ingentaconnect.com/content/dav/aaua/1998/00000084/00000005/art00016.
[26]H. Hudde and A. Engel, "Measuring and modeling basic properties of the human middle ear and ear canal. Part III: Eardrum impedances, transfer functions and model calculations," Acta Acust. Acust. **84**(6), 1091–1108 (1998), https://www.ingentaconnect.com/content/dav/aaua/1998/00000084/00000006/art00015.
[27]M. R. Stinson, E. A. G. Shaw, and B. W. Lawton, "Estimation of acoustical energy reflectance at the eardrum from measurements of pressure distribution in the human ear canal," J. Acoust. Soc. Am. **72**(3), 766–773 (1982).
[28]M. R. Stinson, "The spatial distribution of sound pressure within scaled replicas of the human ear canal," J. Acoust. Soc. Am. **78**(5), 1596–1602 (1985).
[29]J. J. Rosowski, J. T. Cheng, M. E. Ravicz, N. Hulli, M. Hernandez-Montes, E. Harrington, and C. Furlong, "Computer-assisted time-averaged holograms of the motion of the surface of the mammalian tympanic membrane with sound stimuli of 0.4–25 kHz," Hear. Res. **253**(1), 83–96 (2009).
[30]J. Tonndorf and S. M. Khanna, "Tympanic-membrane vibrations in human cadaver ears studied by time-averaged holography," J. Acoust. Soc. Am. **52**(4B), 1221–1233 (1972).
[31]H. Hudde and S. Schmidt, "Sound fields in generally shaped curved ear canals," J. Acoust. Soc. Am. **125**(5), 3146–3157 (2009).
[32]F. Kuk, D. Keenan, and C.-c. Lau, "Comparison of vent effects between a solid earmold and a hollow earmold," J. Am. Acad. Audiol. **20**(8), 480–491 (2009).
[33]A. Winkler, M. Latzel, and I. Holube, "Open versus closed hearing-aid fittings: A literature review of both fitting approaches," Trends Hear. **20**, 1–13 (2016).
[34]K. Carillo, F. Sgard, O. Dazel, and O. Doutres, "Reduction of the occlusion effect induced by earplugs using quasi perfect broadband absorption," Sci. Rep. **12**(1), 15336 (2022).
[35]K. Carillo, F. Sgard, O. Dazel, and O. Doutres, "Passive earplug including Helmholtz resonators arranged in series to achieve broadband near zero occlusion effect at low frequencies," J. Acoust. Soc. Am. **154**(4), 2099–2111 (2023).
[36]S. Stenfelt and R. L. Goode, "Transmission properties of bone conducted sound: Measurements in cadaver heads," J. Acoust. Soc. Am. **118**(4), 2373–2391 (2005).
[37]N. Atalla and F. Sgard, *Finite Element and Boundary Methods in Structural Acoustics and Vibration* (CRC Press, Boca Raton, FL, 2015).
[38]S. Suzuki, S. Maruyama, and H. Ido, "Boundary element analysis of cavity noise problems with complicated boundary conditions," J. Sound Vib. **130**(1), 79–96 (1989).
[39]S. Marburg and R. Anderssohn, "Fluid structure interaction and admittance boundary conditions: Setup of an analytical example," J. Comp. Acoust. **19**(01), 63–74 (2011).
[40]J. Zwislocki, "Analysis of the middle-ear function. Part I: Input impedance," J. Acoust. Soc. Am. **34**(9B), 1514–1523 (1962).
[41]M. R. Stinson and S. M. Khanna, "Sound propagation in the ear canal and coupling to the eardrum, with measurements on model systems," J. Acoust. Soc. Am. **85**(6), 2481–2491 (1989).
[42]M. Lampton, "Transmission matrices in electroacoustics," Acta Acust. Acust. **39**(4), 239–251 (1978), available at https://www.ingentaconnect.com/content/dav/aaua/1978/00000039/00000004/art00005.
[43]R. D. Rabbitt and M. H. Holmes, "Three-dimensional acoustic waves in the ear canal and their interaction with the tympanic membrane," J. Acoust. Soc. Am. **83**(3), 1064–1080 (1988).
[44]J. Lim, I. Dobrev, C. Röösli, S. Stenfelt, and N. Kim, "Development of a finite element model of a human head including auditory periphery for understanding of bone-conducted hearing," Hear. Res. **421**, 108337 (2022).
[45]See https://www.python.org (Last viewed December 21, 2023).
[46]IEC 61260–1:2014, "Electroacoustics—Octave-band and fractional-octave-band filters–Part 1: Specifications" (International Electrotechnical Commission, Geneva, Switzerland, 2014).